Published in final edited form as:

Nat Chem Biol. 2009 March ; 5(3): 157–165. doi:10.1038/nchembio.144.

Golgicide A reveals essential roles for GBF1 in Golgi assembly and function

Jose B. Saenz[1,4], **William J. Sun**[1,4], **Jae Won Chang**[2], **Jinmei Li**[1], **Badry Bursulaya**[3], **Nathanael S. Gray**[2], and **David B. Haslam**[1,*]

[1]Departments of Pediatrics and Molecular Microbiology, Washington University School of Medicine, St. Louis, MO, 63110

[2]Department of Cancer Biology, Dana Farber Cancer Institute, Department of Biological Chemistry and Molecular Pharmacology, Harvard Medical School, Boston, MA, 02115

[3]Genomics Institute of the Novartis Research Foundation, 10675 John Jay Hopkins Drive, San Diego CA 92121

Abstract

ADP-ribosylation factor 1 (Arf1) plays a critical role in regulating secretory traffic and membrane transport within the Golgi of eukaryotic cells. Arf1 is activated by guanine nucleotide exchange factors (ArfGEFs) which confer spatial and temporal specificity to vesicular transport. We describe here the discovery and characterization of Golgicide A (GCA), a potent, highly specific, and reversible inhibitor of the cis-Golgi ArfGEF, GBF1. Inhibition of GBF1 function resulted in rapid dissociation of COPI vesicle coat from Golgi membranes and subsequent disassembly of the Golgi and trans-Golgi network (TGN). Secretion of soluble and membrane-associated proteins was arrested at the ER-Golgi intermediate compartment, whereas endocytosis and recycling of transferrin was unaffected by GBF1 inhibition. Internalized shiga toxin was arrested within the endocytic compartment and was unable to reach the dispersed TGN. Collectively, these results highlight the central role for GBF1 in coordinating bidirectional transport and maintaining structural integrity of the Golgi.

ADP-ribosylation factor proteins, or Arf proteins, are members of the Ras superfamily of small guanosine triphosphatases (GTPases) and mediate vesicular transport in the secretory and endocytic pathways. The Golgi-localized Arf1 is present in all eukaryotic cells and regulates both anterograde and retrograde traffic[1]. As expected for members of the Ras GTPase family, Arf1 cycles between its cytosolic GDP-bound form and its membrane-associated GTP-bound form. In its GTP-bound state, Arf1 recruits adaptor and vesicle coat proteins to initiate the formation and release of transport vesicles. More specifically, Arf1 recruits the heptameric coatomer complex at the *cis*-Golgi face, resulting in assembly of

*Correspondence: haslam@kids.wustl.edu.

[4]These authors contributed equally to this work.

COPI coated vesicles, while clathrin adaptor proteins are recruited to the *trans*-Golgi network (TGN) and endosomes.

The Arf activity cycle is initiated by the interaction of Arf1 with guanine nucleotide exchange factors (GEFs), which exchange GDP for GTP and allow for spatiotemporal activation of Arf1. The ArfGEFS for Arf1 are divided into two families consisting of the large brefeldin A (BFA; **1**)-susceptible molecules, which localize to the Golgi and TGN, and the smaller brefeldin A-resistant ARNO-family GEFs, which predominantly localize to endosomes[2,3]. In mammalian cells, the BFA-susceptible ArfGEFs include GBF1 (Golgi BFA resistance factor 1), a *cis*-Golgi-localized GEF that assists in the recruitment of coat protein COPI[4–6], and BIG1 and BIG2, two functionally similar TGN-localized GEFs that facilitate recruitment of clathrin coat protein[7,8]. Following activation by GBF1, Arf1-mediated COPI coat recruitment enables vesicle transport between the Golgi and endoplasmic reticulum (ER)[9]. Activation by BIG1 and BIG2 results in Arf1 recruitment of adaptor proteins (AP-1, AP-3, and AP-4), which mediate transport between endosomes and either the TGN or lysosomes, and Golgi-associated, gamma adaptin ear containing, Arf-binding proteins (GGA 1–3), monomeric proteins involved in trafficking from the TGN and within the endosomal compartment [10–15].

Recently, the function of individual ArfGEFs has been explored. Among the ArfGEFs, GBF1 has been studied most intensively, either by siRNA-mediated silencing[4,16–18] or by the expression of dominant-negative forms[5,19–21]. The phenotypic and functional effects of these perturbations have not been in complete agreement but nevertheless indicate that GBF1 is essential to intra-Golgi transport. We describe here the discovery and characterization of a potent, highly specific, and rapidly reversible small molecule inhibitor of GBF1 function. This compound, which we called golgicide A (GCA; **2**) reveals diverse and distinct roles for GBF1 in maintaining structure and bidirectional transport through the Golgi and *trans*-Golgi network.

RESULTS

Golgicide A (GCA) is a potent and highly effective inhibitor of shiga toxin activity

From a high-throughput screen for small molecules that inhibit the effect of bacterial toxins on host cells[22], we identified a compound that potently and effectively protected Vero cells from shiga toxin. This compound, which we subsequently named Golgicide A (GCA; Figure 1a), inhibited the effect of shiga toxin on protein synthesis with an IC_{50} of 3.3 μM (Figure 1b). When treated at a concentration of 10 μM, Vero cells where highly protected against the effects of shiga toxin (Figure 1c).

GCA causes reversible dissociation and dispersal of the Golgi and TGN

Other compounds identified in this screen acted through the inhibition of intracellular toxin transport[22], leading us to examine the effect of GCA on toxin trafficking and on intracellular organelle morphology. Immunofluoresence experiments demonstrated dramatic effects of GCA on the Golgi and TGN. Whereas the Golgi remains as a tightly organized perinuclear ribbon in untreated cells, GCA caused complete dispersal of the *medial*-Golgi markers

giantin (Figure 2a) and the cis-Golgi marker GM130 (Figure 2b). These morphological effects on the *cis*- and *medial*-Golgi were highly reminiscent of those caused by brefeldin A (BFA)[23,24]. Time-course experiments revealed that the Golgi initially became extensively tubulated prior to its complete dispersal (Supplemental Figure 1a), similar to the effects of BFA on *cis*- and *medial*-Golgi. Treatment with GCA resulted in a diffuse and punctate distribution of the medial-Golgi marker giantin. The punctate structures were in contact with Sec31-positive foci, indicative of their association with ER exit sites (ERES; Supplemental Figure 1b). These findings were also very similar to BFA which causes Golgi matrix proteins to concentrate at ERES [25]. Effects of these compounds on the TGN, however, were subtly different. Whereas BFA induced the formation of tubules derived from TGN and endosomes, GCA caused the TGN to disperse into small vesicles that subsequently disseminated throughout the cell (Figure 2c and Supplemental Figure 2).

The morphologic effects of GCA did not result from disruption of microtubules or actin cytoskeleton (Supplemental Figure 3). Nor did GCA interfere with transit of transferrin through the endocytic and recycling pathways (Supplemental Figures 4a and 4b). Finally, the effects of GCA were found to be rapidly reversible. Within 15 minutes of removing the compound, the Golgi and TGN began to reassemble (Supplemental Figure 5a). The effects of GCA on protein secretion (Supplemental Figure 5b) were likewise found to be completely reversible within 1 hr of compound removal.

GCA disperses COPI but not AP1 or GGA3 from Golgi membranes

BFA inhibits Arf1 activation, resulting in the rapid dispersal of Golgi-associated vesicle coat proteins COPI and AP-1 at the Golgi and TGN, respectively[26–28]. Since compound GCA had similar effects on the Golgi to BFA, we compared the effects of these compounds on COPI, AP-1 and GGA3 localization. GCA treatment, similar to BFA, resulted in a rapid redistribution of COPI from the Golgi, which was evident within 5 minutes and occurred prior to morphologic changes to Golgi structure and was similar to the effect of BFA (Figure 2d). In contrast, AP-1 (Figure 2e) and GGA3 (Figure 2f) remained associated with the TGN until the Golgi and TGN began to disperse. These results were distinct from those of BFA, which caused rapid dispersal of AP-1 and GGA3 to a diffuse cytoplasmic distribution within minutes of BFA addition.

In summary, GCA and BFA have similar phenotypic effects on *medial*- and *cis*-Golgi which correlate with rapid dispersal of COPI from Golgi membranes. In contrast, these two compounds have differing morphologic effects on the TGN, and have differing effects on AP-1 and GGA3 localization.

Phenotypic effects of GCA are similar to expression of dominant-inactive GBF1

The observation that GCA rapidly dispersed βCOP but not AP1 or GGA3 from Golgi membranes suggested that GCA may specifically target GBF1, the ArfGEF responsible for Arf1 activation and COPI recruitment to *cis*-Golgi membranes, and not affect BIG1 or BIG2, the ArfGEFs responsible for Arf1 activation and vesicle coat recruitment at endosomes and TGN (Figure 3a). Consistent with the possibility that GCA inhibited GBF1 activity, we found that expression of GBF1-E794K, a dominant-inactive GBF1 [21], resulted

in dispersal of βCOP from Golgi membranes and disruption of TGN and *medial*-Golgi structure (Figure 3b), similar to the effects of GCA. The dominant inactive GBF1 was previously shown to localize to the ER-Golgi intermediate compartment (ERGIC) [21], and we found that upon GCA treatment, wild-type GBF1 was largely colocalized with ERGIC-53, a marker for this compartment (Figure 3c). Therefore, treatment with GCA phenotypically resembled expression of dominant-inactive GBF1, further supporting the possibility that GBF1 was the target of GCA.

We next examined the effect of BIG1 overexpression on susceptibility to BFA and GCA. Overexpression of BIG1 was recently shown to partially rescue the effects of BFA on the TGN [16]. We confirmed that BIG1 transfection was partially protective against BFA effects on the TGN (Supplemental Figure 6a) and had no protective effect at the Golgi (Supplemental Figure 6b). By comparison, expression of BIG1 had no protective effect against GCA on either the TGN or Golgi (Supplemental Figures 6a and 6b).

GBF1 is selective for GBF1

In the course of examining the effect of GCA on various cell types, we found that MDCK cells were resistant to GCA as evidenced by a lack of effect of this compound on Golgi morphology and βCOP localization (Supplemental Figure 7a). The Golgi apparatus of MDCK cells has also been reported to be resistant to the effects of BFA[29–31]. Since BFA is known to bind within the highly-conserved Sec7 domain of Golgi-associated ArfGEFs, and because we suspected GBF1 to be the target of GCA, we examined the possibility that differences in the canine GBF1 Sec7 domain accounted for MDCK cell resistance to both compounds. We amplified, cloned, and sequenced the canine GBF1 Sec7 domain. Analysis of several independent clones revealed a leucine substitution for methionine at residue 832 of the full-length protein (numbering corresponds to the human GBF1 sequence). Comparison with all other mammalian GBF1 homologues revealed this substitution to be unique to the canine gene (Supplemental Figure 7b). Interestingly, mutagenesis of the corresponding methionine to leucine in the yeast ArfGEF homologue Gea1 and the human GBF1 resulted in resistance to BFA[32,33].

The M832L substitution was introduced into the hamster GBF1 and the effect of its expression on GCA susceptibility was examined in transfected cells. Vero cells expressing this mutant were highly resistant to GCA, as evidenced by maintenance of βCOP localization, TGN morphology, and *cis*-Golgi structure, even at compound concentrations as high as 100 μM (Figure 4a). As described later, expression of GBF1-M832L rescued the functional effects of GCA on secretion and on retrograde toxin transport. The ability of this mutant to fully protect Vero cells against the phenotypic and functional effects of this compound indicate that GCA specifically targets GBF1 and does not have evident “off-target” effects.

The mechanism of GCA specificity for GBF1 was investigated by molecular modeling and site-directed mutagenesis. The GBF1 Sec7 domain was modeled in complex with Arf1 using the published structure of the Arf1-ARNO-BFA complex[34]. Although there is considerable sequence divergence between GBF1 and BIG1/BIG2 (Figure 4b), the predicted tertiary structure of the GBF1 Sec7 domain is very similar to that of ARNO (Figure 4c). When the

ARNO-Arf1 and predicted GBF1-Arf1 complexes were compared, the BFA-interacting regions of the interfacial cleft were virtually identical. Nevertheless, the observation that the GBF1-M832L mutant was resistant to both BFA and GCA suggested that these compounds may bind within the same GBF1-Arf1 interfacial region. When GCA was docked into this pocket, it was found to extend past the BFA-binding region to contact a tripeptide loop that exists in GBF1 and is lacking in other ArfGEFS, including ARNO, BIG1 and BIG2 (Figure 4c).

The contribution of the GBF1 tripeptide extension to GCA susceptibility was investigated by mutagenesis. Deletion of residues 845 to 848 or substitution of alanines for all three residues resulted in resistance to GCA, as indicated by the ability of these mutants to maintain Golgi morphology in the presence of the compound (Figure 4d). However, as expected, these mutants remained susceptible to BFA (Figure 4d), as this loop lies outside the BFA-binding pocket and would not be expected to contribute to BFA susceptibility (Supplemental Figure 8a). Further mutagenesis of individual residues revealed that substitution of alanine for arginine 843, glutamine 845 or asparagine 846 resulted in loss of susceptibility to GCA, while none of these residues were required for BFA susceptibility (Supplemental Figure 8b). Lysine 844, which protrudes from the opposite side of the GBF1 loop did not affect GCA susceptibility. In summary, these results reveal that GCA susceptibility is dependent upon resides within a tripeptide found within the GBF1 Sec7 domain.

GCA causes a decrease in GBF1-mediated Arf1 activation

GBF1 facilitates the exchange of GDP for GTP on Arf1[5,6]. To determine whether GCA affected GBF1-mediated Arf1 activation, cells were treated with this compound or with BFA and Arf1-GTP was isolated from cellular extracts[35]. GCA caused a consistent and statistically significant decrease of 34% in Arf1 activation *in vivo* (Figure 5). BFA caused a greater decrease in Arf1-GTP (approximating 75% compared to untreated control) which was expected given this compound's more promiscuous effects on ArfGEFs. In order to directly determine whether the effect of GCA on Arf1 activation was due to inhibition of GBF1 function, cells were transduced with the GCA- and BFA-resistant GBF1-M832L mutant and Arf1-GTP levels were assessed in cells treated with these compounds. Whereas GBF1-M832L expression restored Arf1-GTP to approximately 45% of control in BFA-treated cells, Arf1 activation was increased to 86% of control in GCA-treated cells (Figure 5). Interestingly, expression of GBF1-M832L resulted in increased cellular Arf1-GTP levels in untreated cells.

In summary, GCA caused a decrease in Arf1 activation which was attenuated in cells expressing the GCA-resistant mutant. The inability of GBF1-M832L overexpression to completely restore Arf1-GTP levels in GCA-treated cells to the levels of untreated cells was likely because GBF1-M832L expression was not observed in all of the cells (Supplemental Figure 9). BFA caused a much larger decrease in cellular Arf1-GTP and the effect was only partially reversed by the expression of GBF1-M832L. Both of these observations are explained by BFA effects on ArfGEFs other than GBF1. Indeed, these data provide a rough estimate of the relative contribution of GBF1 and other ArfGEFs to cellular Arf1 activation.

These data suggest that in Vero cells growing under tissue culture conditions, GBF1 accounts for approximately 30% of cellular Arf1 activation, BIG1 and BIG2 account for approximately 45%, and BFA-resistant Arf1GEFS such as ARNO, account for the remainder.

Inhibition of GBF1 function arrests secretion of soluble and membrane-anchored proteins

Having demonstrated that GCA was a specific inhibitor of GBF1 function, we used this compound to examine the role of GBF1 in secretory transport. Previous studies with a dominant-inactive mutant indicated that GBF1 function was required for maturation of ER-Golgi intermediate vesicles to a transport-competent state[4,5]. Recent studies with siRNA-mediated inhibition suggested that GBF1 was required for anterograde transport of membrane-anchored cargo but was not required for secretion of soluble molecules[4].

To assess the role of GBF1 in secretion of membrane-anchored proteins, we examined the effect of GCA on transport of a GFP-tagged, temperature sensitive VSV-G mutant, *ts*VSVG-GFP[36]. At the non-permissive temperature of 40°C, this protein is retained and accumulates in the ER. Following a shift to the permissive temperature (32°C), *ts*VSVG-GFP transits through the ERGIC to the Golgi and ultimately to the plasma membrane. Cells were transfected either with *ts*VSVG-GFP alone or co-transfected with plasmid encoding GBF1-WT or GBF1-M832L, and the fate of *ts*VSV-G was followed in GCA-treated cells. In untreated cells, *ts*VSVG-GFP was transported from the ER to Golgi within 60 mins and was located predominantly at the plasma membrane by 4 hrs (Figure 6a). GCA treatment, however, caused *ts*VSVG-GFP to be partially retained in a reticular, ER-like distribution and was also found in diffuse punctate structures (Figure 6b). GBF1-WT overexpression did not overcome the block in *ts*VSVG-GFP secretion in GCA-treated cells, whereas co-transfection with GBF1-M832L restored *ts*VSVG-GFP transport to the plasma membrane (Figure 6c). Expression of the GCA-resistant GBF1 loop mutants also restored transport of (*ts*VSVG-GFP) to the plasma membrane in the presence of GCA (Supplemental Figure 10).

GCA treatment did not completely block *ts*VSVG-GFP transport from the ER, as this protein was also found in peripheral punctate structures after 60 min incubation. These structures were identified as the ER-Golgi intermediate compartment by their labeling with anti-ERGIC53, indicating that *ts*VSVG-GFP was capable of transport from the ER to the ERGIC in cells lacking GBF1 function. (Figure 6d).

To monitor the secretion of soluble cargo proteins, we expressed GFP bearing a neuropeptide Y secretion signal (NPY-GFP)[37]. This protein is secreted from Vero cells with a half life of approximately 60 minutes, as judged by pulse chase experiments[22]. Vero cells expressing NPY-GFP demonstrated markedly decreased GFP secretion in the presence of GCA. If inhibition of NPY-GFP secretion in GCA-treated cells was solely due to the inhibition of GBF1 function, then expression of the GCA-resistant GBF1-M832L mutant should restore protein secretion to levels seen with untreated cells. Therefore, the effect of expressing GBF1-WT or GBF1-M832L on GFP secretion was assessed in GCA-treated cells. Whereas cells transduced with GBF1-WT failed to transport NPY-GFP to the plasma membrane in the presence of GCA, the expression of GBF1-M832L restored of NPY-GFP transport through the Golgi to the plasma membrane (Figure 6e). Together, these findings

reveal that GBF1 function is required for secretion of both soluble and membrane-associated model proteins.

Inhibition of GBF1 function impairs retrograde toxin transport

We next assessed the role of GBF1 in endocytic and retrograde transport pathways by tracking the intracellular fate of cholera toxin (Ctx), shiga toxin (Stx), and transferrin (Tfn). These ligands bind to receptors at the plasma membrane and are transported in retrograde direction to recycling endosomes. From there, Tfn recycles back to the plasma membrane, while Stx and Ctx are transported from endosomes to the TGN, eventually reaching the ER via the Golgi. As described earlier, GCA treatment did not affect the transport of Ctx or Tfn to perinuclear recycling endosomes nor did it affect the rate of Tfn recycling to the plasma membrane. These results indicate that GBF1 function is not required for transport through endocytic transport pathways.

We next examined the effect of GCA on transport of Stx from endosomes to the TGN using a Stx B subunit that bears overlapping tyrosine sulfation sites (StxB-SS)[22]. During its transport through the retrograde transport pathway, this protein is transported from endosomes to the TGN, where it is sulfated by resident tyrosyl-protein sulfotransferases[38,39]. However, treatment with BFA and GCA resulted in marked attenuation of toxin sulfation. Expression of GBF1-WT failed to rescue the transport of StxB-SS to the TGN in BFA and GCA-treated cells. Expression of GBF1-M832L only partially restored toxin sulfation to control levels in BFA-treated cells, presumably because this compound also inhibits BIG1 and BIG2. However, expression of GBF1-M832L completely restored toxin sulfation to control levels in GCA-treated cells (Figure 6f). These results indicate that GBF1 function is required for toxin transport from endosomes to the TGN. Whether GBF1 functions directly in endosome-to-TGN transport, or indirectly through its effects on maintaining Golgi structure, is currently unknown.

GCA was identified in a high-throughput screen for its ability to inhibit the effects of shiga toxin on mammalian cells. The data presented thus far indicate that retrograde toxin transport was arrested within the endocytic compartment. To determine whether the effects of GCA on toxin transport were due solely to GBF1 inhibition, we examined the ability of GBF1-M832L to restore toxin susceptibility to GCA-treated cells. Cells were transduced with the appropriate GBF1 constructs and treated with GCA. Toxin susceptibility was highly attenuated in control cells and those transduced with GBF1-WT. In contrast, Stx susceptibility was fully restored in GCA-treated cells expressing GBF1-M832L, indicating that the effects of GCA on toxin susceptibility were solely due to GBF1 inhibition (Figure 6g). Together, these results indicate that GBF1 function is not required for transport of bacterial toxins to recycling endosomes, but this ArfGEF is required for retrograde transport of Stx from endosomes to the TGN and Golgi.

DISCUSSION

Phenotypic screens aimed at identifying inhibitors of endocytic and secretory transport have uncovered small molecules that are highly useful probes of intracellular transport. Exo1 (**3**)[40] and Exo2 (**4**)[41] were uncovered from an image-based screen for inhibitors of secretory

transport and exhibited Golgi-disruptive effects. Studies with Exo2 revealed that treatment with this compound ablated the Golgi but maintained TGN integrity and suggested the existence of an alternative pathway for cholera toxin transport. Exo1 exhibited BFA-like effects on Arf1 dissociation from Golgi membranes, but unlike BFA, it did not interfere with ArfGEF activity. A high-throughput screen for inhibitors of dynamin GTPase activity discovered dynasore (**5**), a particularly useful probe for studying the dynamics of dynamin-mediated clathrin coat formation[42,43]. Similarly, secramine (**6**) was identified as a novel tool for dissecting the functions of Cdc42 and possibly other RhoGTPases[44]. Finally, SecinH3 (**7**), an inhibitor of the cytoadhesins was recently identified and its use revealed a role for these BFA-insensitive ArfGEFs in insulin signaling[45]. Together, these studies underscore the utility of small molecules as biological probes for dynamic intracellular processes.

Herein we describe the identification and characterization of golgicide A (GCA), a potent, highly effective, and rapidly reversible inhibitor of GBF1. Mutagenesis and molecular modeling revealed that GCA binds within the an interfacial cleft formed between Arf1 and the GBF1 Sec7 domain. Interestingly, BFA binds within this cleft[46,47] and substitution of methionine 832 to leucine results in resistance to BFA [33,32], as well as to GCA. However, GCA extends beyond the BFA-binding cleft to contact a tripeptide loop present in GBF1 but lacking from all other known Arf1GEFS, accounting for its selectivity.

Having demonstrated the highly selective nature of GCA activity, we used the compound to delineate the role of GBF1 in anterograde and retrograde transport through the Golgi. We found that transport of *ts*VSVG-GFP was arrested in the ER-Golgi intermediate compartment, indicating that GBF1 function was not required for exit of cargo from the ER, but was required for transport past the ERGIC. These results are similar to those found with expression of a dominant-negative GBF1 and by siRNA-mediated inhibition of GBF1[48]. Inhibition of GBF1 function with GCA also blocked secretion of GFP bearing a secretion signal. This finding differs from RNAi-based studies which found relatively mild effects of GBF1 inhibition on Golgi morphology and which suggested GBF1 was not required for secretion of soluble cargo[4]. The relatively milder effects of GBF1 inhibition by RNAi likely resulted from less than complete inhibition of GBF1 expression, as functional inhibition by GCA resulted in marked disruption of Golgi morphology and an absolute block in secretion of soluble and transmembrane proteins.

The role of GBF1 in retrograde transport to the Golgi has not previously been investigated. We demonstrate that endocytic cargo is transported normally through recycling endosomes in the presence of GCA, indicating that GBF1 function is not required for these pathways. However, upon inhibition of GBF1 function, bacterial toxins are trapped in the endocytic compartment and are unable to reach the dispersed TGN, indicating that GBF1 function is required to maintain communication between endosomes and the TGN.

In summary, GCA revealed essential roles for GBF1 in maintaining Golgi structure and enabling anterograde and retrograde traffic through the Golgi and TGN. Given its specificity, efficacy, and reversibility, GCA will be a unique and powerful tool to further elucidate the mechanisms underlying assembly and transport within the Golgi.

METHODS

Chemical characterization of GCA

GCA was identified from a commercial compound library available from ChemDiv. Analysis of the screening DMSO solution by reverse-phase LC-MS revealed the compound to be present as a 10:1 diastereomeric mixture. The compound was resynthesized using a published procedure (Supplementary Methods) which also resulted in a 10:1 diastereomeric mixture which was determined to be identical to that obtained from the screening library by ^{1}H NMR and LC-MS. Purification of the major isomer was achieved by recrystallization from acetonitrile and water. The biological activity of this purified major isomer was identical to the material obtained from the library DMSO solution. The calculated molecular weight is 284.3. ^{1}H NMR 600 MHz ($CDCl_3$) δ 8.78 (*d*, *J* = 1.5 Hz, 1H), 8.62 (*dd*, *J* = 1.2, 3.8 Hz, 1H), 8.03 (*d*, *J* = 7.9 Hz, 1H), 7.52 (*m*, 1H), 6.63 (*m*, 2H), 5.83 (*m*, 1H), 5.69 (*m*, 1H), 4.70 (*d*, *J* = 2.9 Hz, 1H), 4.10 (*d*, J = 8.5 Hz, 1H), 3.95 (*s*, 1H), 3.00 (*m*, 1H), 2.59 (*m*, 1H), 1.82 (*m*, 1H); ^{13}C NMR 150 MHz ($CDCl_3$) δ 147.7, 147.2, 138.7, 135.8, 133.0, 132.2, 131.1, 124.3, 110.4, 110.3, 101.3, 101.2, 101.1, 55.6, 46.2, 45.6, 31.3; MS *m/z* 285.19 (M + 1).

Radioactive protein synthesis assay

The luciferase-based high-throughput screen to identify inhibitors of Stx trafficking has previously been described[22,49] Confirmation of positive hits from the ChemDiv4 library screen was assessed by a previously described radioactiveassay[22] and is described in Supplementary Methods.

Immunofluorescence

For all immunofluorescence experiments, cells were fixed in 4% paraformaldehyde in cold PBS, permeabilized with 0.1% Triton X-100 in PBS, blocked, then probed with primary and secondary (Alexa Fluor 488 or 594-labeled donkey anti-IgG) antibodies diluted in blocking buffer (DMEM containing 10% fetal calf serum plus, 1 mg/ml BSA). Cells were rinsed thoroughly in PBS prior to mounting in SlowFade Gold reagent containing DAPI. Fluorescence imaging used epifluorescence (Zeiss) microscopy.

Cloning, sequence analysis, site-directed mutagenesis and generation of adenoviral expression constructs

The hamster GBF1 cDNA (a gift from Paul Melançon, University of Alberta, Edmonton, AB) was used as template for constructing HA-tagged wild-type and mutant cDNA. Methods and primer sequences for cloning of canine GBF1 Sec7 domain, mutagenesis of GBF1, and generation of adenoviral constructs is described in Supplementary Methods.

Arf1-GTP pulldown assay

Was performed with human Arf1 and the VHS and GAT domains of human GGA3, cloned as purified described in Supplementary Methods. The pulldown assay followed a published protocol[35] with modifications as described in Supplementary Methods.

Molecular Modeling of GBF1-Arf1-GCA complex

The GBF1 homology model was built using Prime 2.0 software from FirstDiscovery suite (Schrodinger, LLC, Portland, OR) and ARNO coordinates from ARNO-Arf1 complex (PDB id 1r8q) as a template[34]. Fully flexible ligand docking was performed with Glide 5.0 (Schrodinger, LLC, Portland, OR). The protein was prepared for grid generation and subsequent docking using the Protein Preparation Wizard tool from FirstDiscovery suite. The default settings for grid calculations and docking were used. Images were created with UCSF Chimera version 1.2540 for Windows[50].

Toxin and transferrin internalization

For CtxB and transferrin trafficking experiments, Vero cells grown in chamber slides (2.5×10^4 cells/chamber) were treated with serum-free medium containing DMSO, GCA, or BFA at the indicated concentrations and times at 37°C. Following the binding of toxin and transferrin at 4°C, cells were shifted to 19°C for 1 h to allow for toxin internalization. Cells were processed for immunofluorescence as described above.

Trafficking of tsVSVG-GFP, NPY-GFP secretion, and StxB-SS-His sulfation assays

Transport of tsVSVG-GFP[36], secretion of NPY-GFP[22], and sulfation of StxB-SS-His[22] were performed using published protocols with modifications as described in Supplementary Methods.

Supplementary Material

Refer to Web version on PubMed Central for supplementary material.

Acknowledgments

The authors wish to thank Su Chiang and the ICCB-Longwood staff for their assistance with screening, Jennifer Loughman for synthesis of MDCK cell cDNA, Paul Melançon for providing the hamster GBF1 cDNA, Martha Vaughn for providing the BIG1-HA cDNA, Matthew Haslam for technical assistance and Stuart Kornfeld and Guojon Bu for advice and critical review of the manuscript. This work was supported by National Institutes of Health grant U54 AI057160 to the Midwest Regional Center of Excellence for Biodefense and Emerging Infectious Diseases Research (MRCE) and an Investigators in Microbial Pathogenesis Award from the Burroughs Wellcome Foundation.

References

1. Donaldson JG, Honda A, Weigert R. Multiple activities for Arf1 at the Golgi complex. Biochim Biophys Acta. 2005; 1744:364–73. [PubMed: 15979507]
2. Cohen LA, et al. Active Arf6 recruits ARNO/cytohesin GEFs to the PM by binding their PH domains. Mol Biol Cell. 2007; 18:2244–53. [PubMed: 17409355]
3. Shmuel M, et al. ARNO through its coiled-coil domain regulates endocytosis at the apical surface of polarized epithelial cells. J Biol Chem. 2006; 281:13300–8. [PubMed: 16484220]
4. Szul T, et al. Dissecting the role of the ARF guanine nucleotide exchange factor GBF1 in Golgi biogenesis and protein trafficking. J Cell Sci. 2007; 120:3929–40. [PubMed: 17956946]
5. Zhao X, et al. GBF1, a cis-Golgi and VTCs-localized ARF-GEF, is implicated in ER-to-Golgi protein traffic. J Cell Sci. 2006; 119:3743–53. [PubMed: 16926190]
6. Claude A, et al. GBF1: A novel Golgi-associated BFA-resistant guanine nucleotide exchange factor that displays specificity for ADP-ribosylation factor 5. J Cell Biol. 1999; 146:71–84. [PubMed: 10402461]

7. Pacheco-Rodriguez G, Moss J, Vaughan M. BIG1 and BIG2: brefeldin A-inhibited guanine nucleotide-exchange proteins for ADP-ribosylation factors. Methods Enzymol. 2002; 345:397–404. [PubMed: 11665623]
8. Shinotsuka C, Waguri S, Wakasugi M, Uchiyama Y, Nakayama K. Dominant-negative mutant of BIG2, an ARF-guanine nucleotide exchange factor, specifically affects membrane trafficking from the trans-Golgi network through inhibiting membrane association of AP-1 and GGA coat proteins. Biochem Biophys Res Commun. 2002; 294:254–60. [PubMed: 12051703]
9. Bonifacino JS, Glick BS. The mechanisms of vesicle budding and fusion. Cell. 2004; 116:153–66. [PubMed: 14744428]
10. Boehm M, Aguilar RC, Bonifacino JS. Functional and physical interactions of the adaptor protein complex AP-4 with ADP-ribosylation factors (ARFs). Embo J. 2001; 20:6265–76. [PubMed: 11707398]
11. Robinson MS. Adaptable adaptors for coated vesicles. Trends Cell Biol. 2004; 14:167–74. [PubMed: 15066634]
12. Boman AL, Zhang C, Zhu X, Kahn RA. A family of ADP-ribosylation factor effectors that can alter membrane transport through the trans-Golgi. Mol Biol Cell. 2000; 11:1241–55. [PubMed: 10749927]
13. Dell'Angelica EC, et al. GGAs: a family of ADP ribosylation factor-binding proteins related to adaptors and associated with the Golgi complex. J Cell Biol. 2000; 149:81–94. [PubMed: 10747089]
14. Doray B, Ghosh P, Griffith J, Geuze HJ, Kornfeld S. Cooperation of GGAs and AP-1 in packaging MPRs at the trans-Golgi network. Science. 2002; 297:1700–3. [PubMed: 12215646]
15. Ghosh P, Kornfeld S. The GGA proteins: key players in protein sorting at the trans-Golgi network. Eur J Cell Biol. 2004; 83:257–62. [PubMed: 15511083]
16. Manolea F, Claude A, Chun J, Rosas J, Melancon P. Distinct Functions for Arf Guanine Nucleotide Exchange Factors at the Golgi Complex: GBF1 and BIGs Are Required for Assembly and Maintenance of the Golgi Stack and trans-Golgi Network, Respectively. Mol Biol Cell. 2008; 19:523–35. [PubMed: 18003980]
17. Citterio C, et al. Unfolded protein response and cell death after depletion of brefeldin A-inhibited guanine nucleotide-exchange protein GBF1. Proc Natl Acad Sci U S A. 2008
18. Lefrancois S, McCormick PJ. The Arf GEF GBF1 is required for GGA recruitment to Golgi membranes. Traffic. 2007; 8:1440–51. [PubMed: 17666033]
19. Holloway ZG, et al. Activation of ADP-ribosylation factor (Arf) regulates biogenesis of the ATP7A containing trans-Golgi network compartment and its Cu-induced trafficking. Am J Physiol Cell Physiol. 2007
20. Monetta P, Slavin I, Romero N, Alvarez C. Rab1b interacts with GBF1 and modulates both ARF1 dynamics and COPI association. Mol Biol Cell. 2007; 18:2400–10. [PubMed: 17429068]
21. Szul T, et al. Dissection of membrane dynamics of the ARF-guanine nucleotide exchange factor GBF1. Traffic. 2005; 6:374–85. [PubMed: 15813748]
22. Saenz JB, Doggett TA, Haslam DB. Identification and characterization of small molecules that inhibit intracellular toxin transport. Infect Immun. 2007; 75:4552–61. [PubMed: 17576758]
23. Lippincott-Schwartz J, et al. Microtubule-dependent retrograde transport of proteins into the ER in the presence of brefeldin A suggests an ER recycling pathway. Cell. 1990; 60:821–36. [PubMed: 2178778]
24. Doms RW, Russ G, Yewdell JW. Brefeldin A redistributes resident and itinerant Golgi proteins to the endoplasmic reticulum. J Cell Biol. 1989; 109:61–72. [PubMed: 2745557]
25. Puri S, Linstedt AD. Capacity of the golgi apparatus for biogenesis from the endoplasmic reticulum. Mol Biol Cell. 2003; 14:5011–8. [PubMed: 14565973]
26. Presley JF, et al. Dissection of COPI and Arf1 dynamics in vivo and role in Golgi membrane transport. Nature. 2002; 417:187–93. [PubMed: 12000962]
27. Liu W, Duden R, Phair RD, Lippincott-Schwartz J. ArfGAP1 dynamics and its role in COPI coat assembly on Golgi membranes of living cells. J Cell Biol. 2005; 168:1053–63. [PubMed: 15795316]

28. Helms JB, Rothman JE. Inhibition by brefeldin A of a Golgi membrane enzyme that catalyses exchange of guanine nucleotide bound to ARF. Nature. 1992; 360:352–4. [PubMed: 1448152]
29. Sandvig K, Prydz K, Hansen SH, van Deurs B. Ricin transport in brefeldin A-treated cells: correlation between Golgi structure and toxic effect. J Cell Biol. 1991; 115:971–81. [PubMed: 1955466]
30. Prydz K, Hansen SH, Sandvig K, van Deurs B. Effects of brefeldin A on endocytosis, transcytosis and transport to the Golgi complex in polarized MDCK cells. J Cell Biol. 1992; 119:259–72. [PubMed: 1400572]
31. Hunziker W, Whitney JA, Mellman I. Selective inhibition of transcytosis by brefeldin A in MDCK cells. Cell. 1991; 67:617–27. [PubMed: 1934063]
32. Niu TK, Pfeifer AC, Lippincott-Schwartz J, Jackson CL. Dynamics of GBF1, a Brefeldin A-sensitive Arf1 exchange factor at the Golgi. Mol Biol Cell. 2005; 16:1213–22. [PubMed: 15616190]
33. Peyroche A, et al. Brefeldin A acts to stabilize an abortive ARF-GDP-Sec7 domain protein complex: involvement of specific residues of the Sec7 domain. Mol Cell. 1999; 3:275–85. [PubMed: 10198630]
34. Renault L, Guibert B, Cherfils J. Structural snapshots of the mechanism and inhibition of a guanine nucleotide exchange factor. Nature. 2003; 426:525–30. [PubMed: 14654833]
35. Santy LC, Casanova JE. Activation of ARF6 by ARNO stimulates epithelial cell migration through downstream activation of both Rac1 and phospholipase D. J Cell Biol. 2001; 154:599–610. [PubMed: 11481345]
36. Hirschberg K, et al. Kinetic analysis of secretory protein traffic and characterization of golgi to plasma membrane transport intermediates in living cells. J Cell Biol. 1998; 143:1485–503. [PubMed: 9852146]
37. El Meskini R, et al. A signal sequence is sufficient for green fluorescent protein to be routed to regulated secretory granules. Endocrinology. 2001; 142:864–73. [PubMed: 11159860]
38. Lin WH, Larsen K, Hortin GL, Roth JA. Recognition of substrates by tyrosylprotein sulfotransferase. Determination of affinity by acidic amino acids near the target sites. J Biol Chem. 1992; 267:2876–9. [PubMed: 1737745]
39. Niehrs C, Huttner WB. Purification and characterization of tyrosylprotein sulfotransferase. Embo J. 1990; 9:35–42. [PubMed: 2295314]
40. Feng Y, et al. Exo1: a new chemical inhibitor of the exocytic pathway. Proceedings of the National Academy of Sciences of the United States of America. 2003; 100:6469–74. [PubMed: 12738886]
41. Feng Y, et al. Retrograde transport of cholera toxin from the plasma membrane to the endoplasmic reticulum requires the trans-Golgi network but not the Golgi apparatus in Exo2-treated cells. EMBO Reports. 2004; 5:596–601. [PubMed: 15153932]
42. Newton AJ, Kirchhausen T, Murthy VN. Inhibition of dynamin completely blocks compensatory synaptic vesicle endocytosis. Proc Natl Acad Sci U S A. 2006; 103:17955–60. [PubMed: 17093049]
43. Macia E, et al. Dynasore, a cell-permeable inhibitor of dynamin. Dev Cell. 2006; 10:839–50. [PubMed: 16740485]
44. Pelish HE, et al. Secramine inhibits Cdc42-dependent functions in cells and Cdc42 activation in vitro. Nat Chem Biol. 2006; 2:39–46. [PubMed: 16408091]
45. Hafner M, et al. Inhibition of cytohesins by SecinH3 leads to hepatic insulin resistance. Nature. 2006; 444:941–4. [PubMed: 17167487]
46. Zeeh JC, et al. Dual specificity of the interfacial inhibitor brefeldin a for arf proteins and sec7 domains. J Biol Chem. 2006; 281:11805–14. [PubMed: 16484231]
47. Renault L, Christova P, Guibert B, Pasqualato S, Cherfils J. Mechanism of domain closure of Sec7 domains and role in BFA sensitivity. Biochemistry. 2002; 41:3605–12. [PubMed: 11888276]
48. Garcia-Mata R, Szul T, Alvarez C, Sztul E. ADP-ribosylation factor/COPI-dependent events at the endoplasmic reticulum-Golgi interface are regulated by the guanine nucleotide exchange factor GBF1. Mol Biol Cell. 2003; 14:2250–61. [PubMed: 12808027]

49. Zhao L, Haslam DB. A quantitative and highly sensitive luciferase-based assay for bacterial toxins that inhibit protein synthesis. Journal of Medical Microbiology. 2005; 54:1023–30. [PubMed: 16192432]

50. Pettersen EF, et al. UCSF Chimera--a visualization system for exploratory research and analysis. J Comput Chem. 2004; 25:1605–12. [PubMed: 15264254]

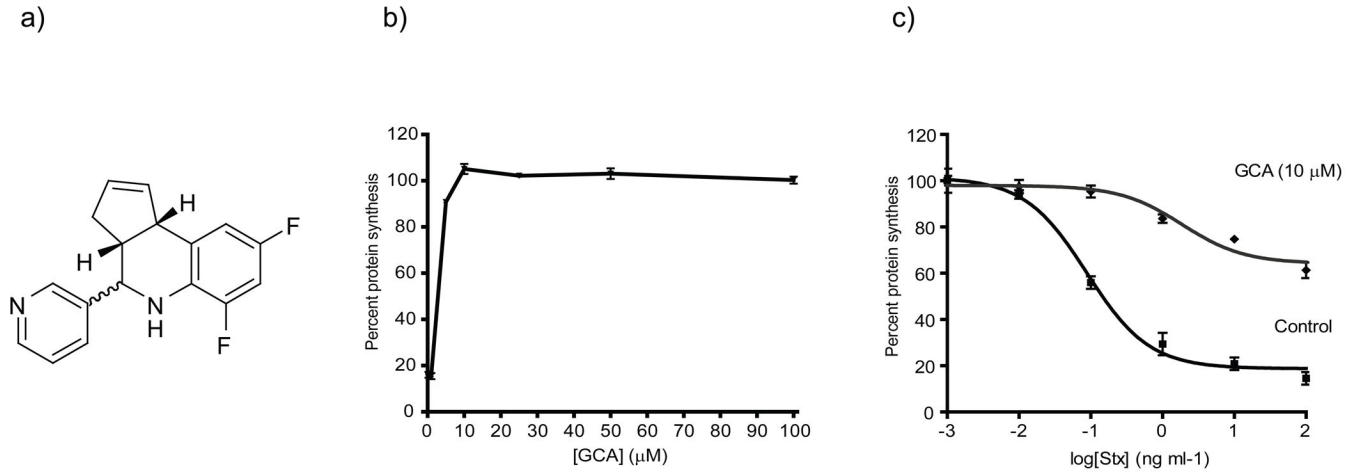

Figure 1.

Discovery of GCA as a potent and effective inhibitor of Stx susceptibility. (a) Structure of GCA. (b) Vero cells were pretreated for 30 min at 37°C with varying concentrations of GCA, followed by incubation with Stx (1 ng/mL) for 4 h at 37°C. % Protein synthesis indicates the amount of radioactive amino acid incorporation in GCA-treated cells as a percentage of radioactive amino acid incorporation in cells lacking Stx treatment (control). Protein synthesis levels and compound-response curves were determined as described in Methods. (c) Protein synthesis levels for control (squares; no compound) or GCA-treated (triangles; 10 μM) Vero cells were determined using the radioactive amino acid incorporation assay as described in (b). % Protein synthesis is expressed as the amount of radioactive amino acid incorporation in untreated or GCA-treated cells at a given toxin concentration as a percentage of radioactive amino acid incorporation in cells lacking Stx treatment. Toxin IC_{50} values for GCA-treated cells were significantly increased over control cells ($p<0.01$; see Methods). For (a) and (b), data points (mean ±SD) represent triplicate data at the indicated compound or toxin concentrations, respectively, from one representative experiment. Stx, Shiga toxin; GCA, golgicide A.

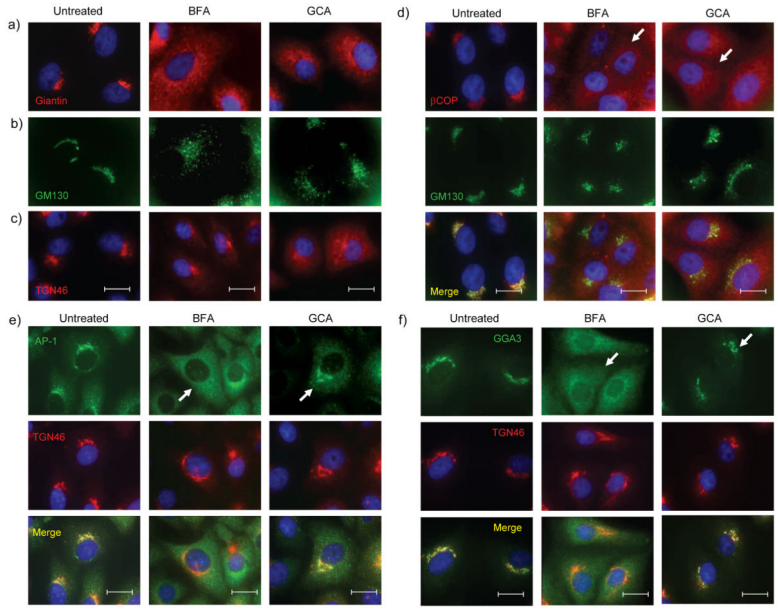

Figure 2.

GCA disperses *medial*- and *cis*-Golgi, inhibits COPI recruitment, and maintains localization of AP-1 and GGA3 to TGN. (a,b) Vero cells were either left untreated or treated with BFA (10 μg/mL) or GCA (10 μM) for 1 hr, and the localization of (a) giantin (*medial*-Golgi), (b) GM130 (*cis*-Golgi), and (c) TGN46 (TGN) were determined (see Methods). The distribution of *medial*- and *cis*-Golgi was similar in BFA- and GCA-treated cells, while GCA did not induce tubulation of the TGN as observed in BFA-treated cells. (d) Vero cells treated for 5 min with BFA (10 μg/mL) or GCA (10 μM) show dispersed COPI staining (arrows) that does not colocalize with the Golgi (green) as in untreated cells. (e,f) Unlike BFA, GCA maintains (e) AP-1 and (f) GGA3 association with the TGN after 5 min of treatment (see arrows). BFA, brefeldin A; blue, nuclei. White scale bars = 20 μm.

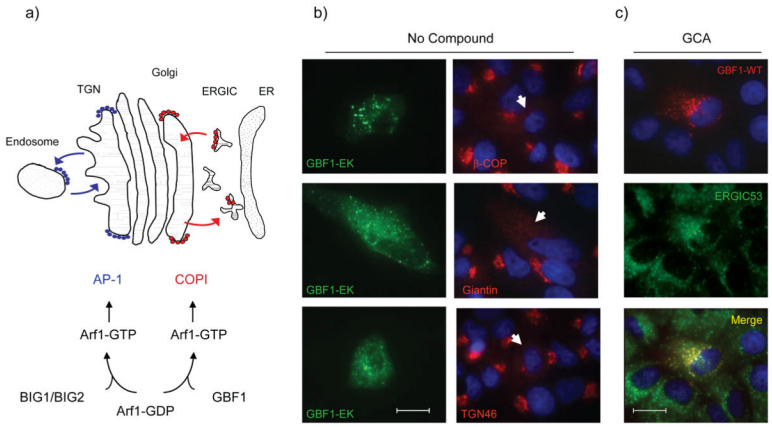

Figure 3.

The effects of GCA are similar to expression of inactive GBF1-E794K. (a) Schematic diagram of the roles of GBF1 and BIG1/BIG2 in Arf1 activation. Arf1 in the inactive (GDP-bound) form is localized to the cytoplasm. Exchange of GDP for GTP by either BIG1/2 or GBF1 results in local Arf1 activation, membrane localization, and subsequent recruitment of vesicle coat proteins such as AP-1 or COPI. (b) Vero cells expressing the GBF1-EK mutant show dispersal of β-COP, the *medial*-Golgi (giantin), and the *trans*-Golgi network (TGN46). Arrows indicate the effect of GBF1-E794K expression on giantin, βCOP, or TGN46 localization. Blue, nuclei. (c) GBF1-WT is predominantly membrane-associated in GCA-treated cells and distributed to punctate structures that co-label with anti-ERGIC53. White scale bars = 20 μm.

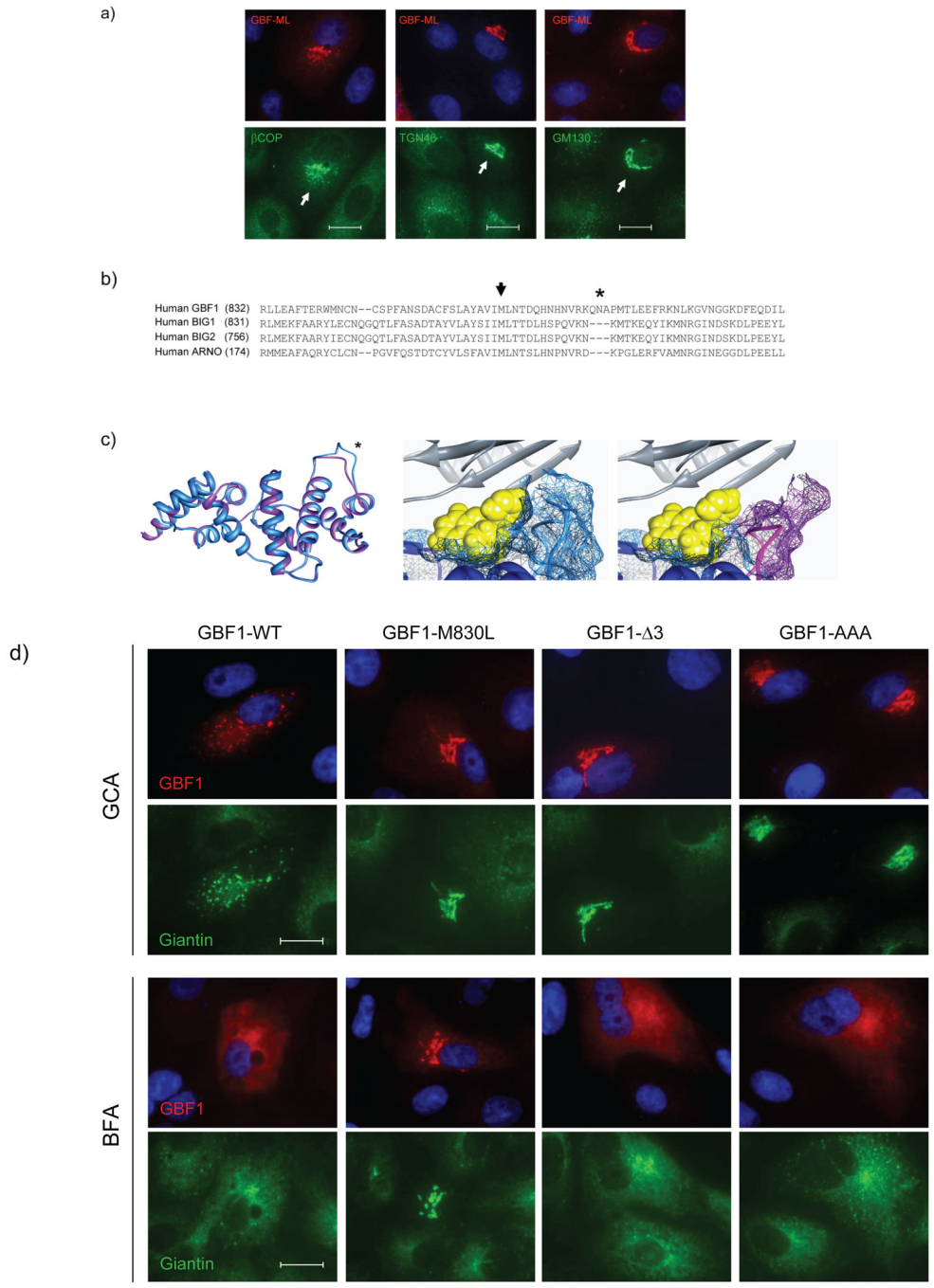

Figure 4.

GCA is selective for GBF1 (a) Expression of GBF1-M832L (GBF1-ML) results in protection from the effects of GCA. Vero cells were transiently transfected with GBF1-ML and exposed to 100 μM GCA. β-COP, TGN46, and GM130 localization were resistant to the effects of GCA. Arrows indicate cells expressing GBF1-ML. Blue, nuclei. White scale bars = 20 μm. (b) Comparison of the amino acid sequence of Sec7 domains reveals considerable divergence between GBF1 and BIG1/BIG2. Particularly notable was the presence of three extra residues in the GBF1 sequence (asterisk) (c) The GBF1 Sec7 domain (residues 693 to

887) was thread on the previously reported ARNO-Arf1-BFA complex. Only the Sec7 domains of GBF1 (blue) and ARNO (purple) are shown (left panel). The modeled tertiary structures are nearly identical, with the exception of an additional loop in the GBF1 Sec7 domain (asterisk), corresponding to the tripeptide insertion in GBF1 sequence. GCA was docked into the BFA binding pocket, revealing the compound to extend past the BFA-binding region to make contact with the GBF1 tripeptide loop (middle panel; light blue). In these images, predicted molecular surfaces are indicated by colored mesh around the ribbon backbone. The corresponding region of ARNO, BIG1 and BIG2 lacks the tripeptide (right panel, purple) and does not contact GCA. In these images, GCA is yellow and Arf1 ribbon diagram is gray. (d) Mutagenesis of the tripeptide, either by deletion of the three residues, or alteration to three alanine residues results in resistance to GCA but not BFA. Cells were transiently transfected either with GBF1-WT, GBF1-ML, GBF1-Δ3 (QNV deleted), or GBF1-AAA (QNV to AAA) then exposed to GCA (10 μM; top panel) or BFA (10 μg/ml; bottom panel) for 1 hr, and labeled with antibodies against HA and giantin. White scale bars = 20 μm.

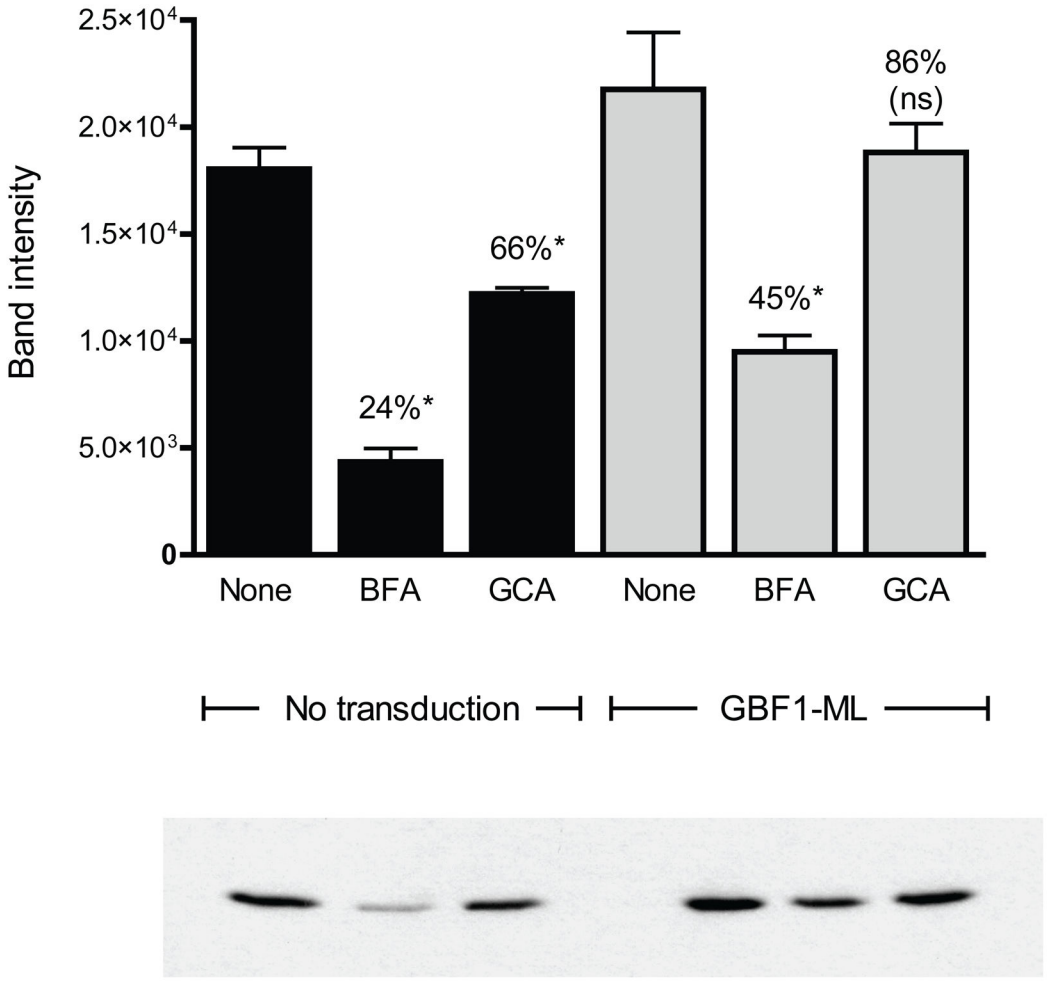

Figure 5.

GCA causes a decrease in GBF1-dependent Arf1 activation. Vero cells transduced with Arf1-V5 alone or Arf1-V5 plus GBF1-M832L-HA were exposed either to no compound (Untreated), BFA (10 μg/ml) or GCA (10 μM) for 1 hr. The cells were then lysed and extracts incubated with immobilized GST-GGA3. Bound proteins were released and separated by SDS-PAGE. Arf1-V5 was detected by Western blot and band intensity was determined using ImageJ software. Statistical analysis was performed on duplicate experiments. (*, statistically significant from untreated sample [P=0.05]; ns, not statistically significantly different from untreated sample).

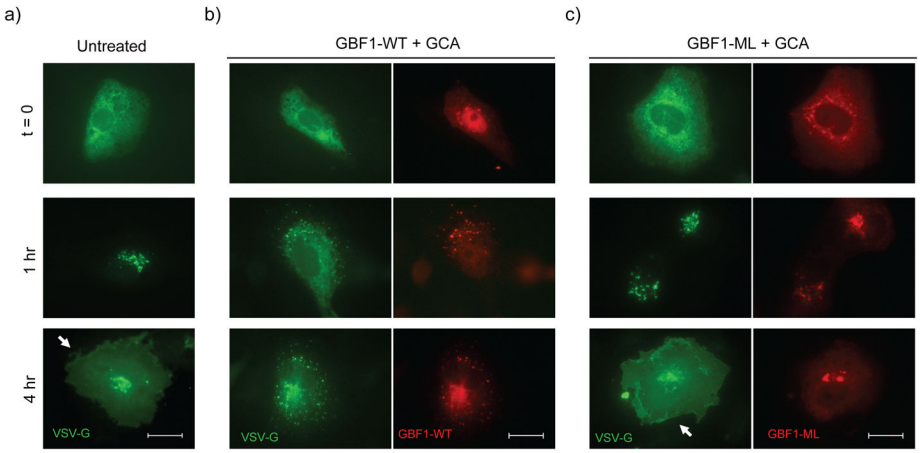

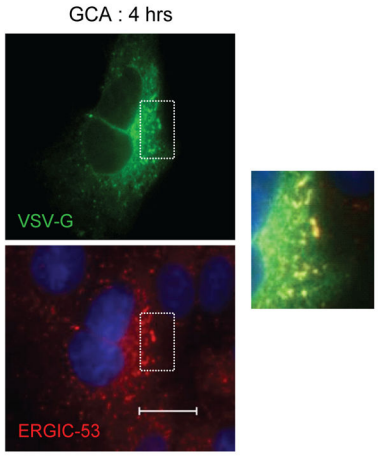

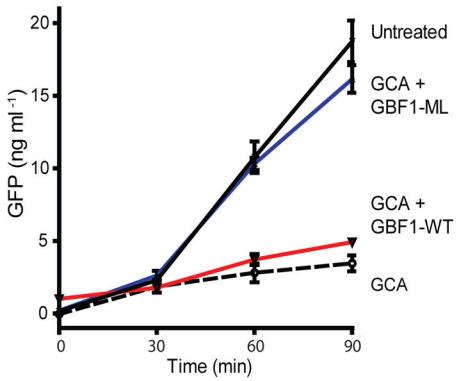

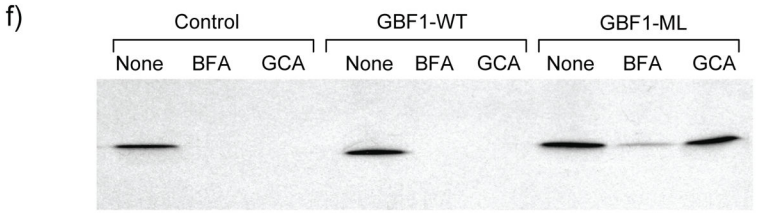

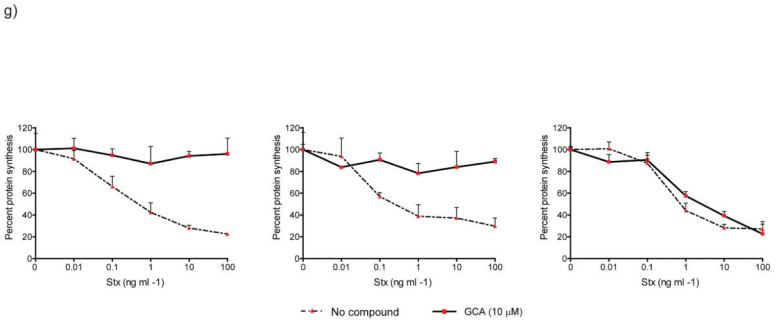

Figure 6.

GBF1 inhibition arrests secretion of membrane-anchored and soluble proteins. Trafficking of *ts*VSVG-GFP (green) was arrested in GCA-treated cells. Vero cells were co-transfected with *ts*VSVG-GFP and either (a) no additional plasmid, (b) wild-type GBF1 (GBF1-WT), or (c) the GBF1-M832L mutant (GBF1-ML). The cells were incubated at 40°C to trap *ts*VSVG-GFP in the ER, followed by treatment with either (a) no compound or (b,c) GCA (10 μM) prior to shifting the cells to 32°C. At various times (t = 0, 1, and 4 h) following the temperature shift, cells were fixed and labeled with anti-HA antibody (GBF1 proteins; red). Expression of the GBF1-ML mutant restored *ts*VSVG-GFP transit to the plasma membrane (arrow). (d) *ts*VSVG-GFP co-localizes with ERGIC53 in GCA-treated cells. Vero cells transfected with tsVSVG-GFP were incubated at 40°C before a shift to 32°C for 4 h in the presence of GCA (10 μM). The cells were fixed and labeled with an anti-ERGIC53 antibody (red). Inset shows magnification of boxed area and co-localization of VSVG with the ERGIC (yellow). Blue, nuclei. White scale bars = 20 μm. (e) GCA inhibits secretion of soluble cargo. Cells were transduced either with adenovirus expressing NPY-GFP alone or co-transduced with NPY-GFP plus adenovirus expressing GBF1-WT or GBF1-ML. The cells were either left untreated or were exposed to GCA (10 μM) for 1 h. At various times, the media was removed and GFP concentration assessed by ELISA (see Supplementary Methods). GCA treatment decreases NPY-GFP secretion in untransduced cells (dotted), while overexpression of GBF1-ML (blue), but not GBF1-WT (red), restores NPY-GFP secretion to levels in untransduced, untreated cells (black). (f) Sulfation of a StxB construct with a tandem of sulfation sites (StxB-SS) was used to assess trafficking from endosomes to the TGN. Control Vero cells, or those transduced with GBF1-WT or GBF1-ML were preincubated with no compound, BFA (10 μg/ml) or GCA (10 μM), then StxB-SS was added for 3 hrs in the presence of $[^{35}S]O_4$ as described in Supplementary Methods. StxB-SS was recovered from cell lysates and subjected to SDS-PAGE and autoradiography to detect radiolabeled toxin. (g) Inhibition of shiga toxicity by GCA is completely reversed in cells expressing GBF1-ML. Cells were either left untransduced or transduced with adenovirus expressing GBF1-WT or GBF1-ML and were exposed either to GCA (solid line) or no compound (dotted line) prior to treatment with increasing concentrations of Stx. After 4 h incubation, protein synthesis was assessed, as described in Supplementary Methods. GBF1-ML expression restores Stx susceptibility in GCA-treated cells.